PHILOSOPHICAL TRANSACTIONS A

rsta.royalsocietypublishing.org

Research

Cite this article: Svensen HH, Frolov S, Akhmanov GG, Polozov AG, Jerram DA, Shiganova OV, Melnikov NV, Iyer K, Planke S. 2018 Sills and gas generation in the Siberian Traps. *Phil. Trans. R. Soc. A* **376**: 20170080. http://dx.doi.org/10.1098/rsta.2017.0080

Accepted: 29 May 2018

One contribution of 11 to a discussion meeting issue 'Hyperthermals: rapid and extreme global warming in our geological past'.

Subject Areas:
geology

Keywords:
Siberian traps, large igneous provinces, End-Permian

Author for correspondence:
Henrik H. Svensen
e-mail: hensven@geo.uio.no

Electronic supplementary material is available online at https://dx.doi.org/10.6084/m9.figshare.c.4179029.

THE ROYAL SOCIETY PUBLISHING

Sills and gas generation in the Siberian Traps

Henrik H. Svensen[1], Sergei Frolov[2], Grigorii G. Akhmanov[2], Alexander G. Polozov[1,3], Dougal A. Jerram[1,4], Olga V. Shiganova[5], Nikolay V. Melnikov[5], Karthik Iyer[6,7] and Sverre Planke[1,8]

[1]Centre for Earth Evolution and Dynamics (CEED), University of Oslo, Oslo, Norway
[2]Faculty of Geology, Lomonosov Moscow State University, Moscow, Russia
[3]Institute of Geology of Ore Deposits, Petrography, Mineralogy and Geochemistry, Russian Academy of Sciences (IGEM RAS), Moscow, Russia
[4]DougalEARTH Ltd., Solihull, UK
[5]Siberian Scientific Research Institute of Geology, Geophysics and Mineral Resources, Novosibirsk, Russia
[6]GeoModelling Solutions GmbH, Zurich, Switzerland
[7]GEOMAR, Helmholtz Centre for Ocean Research, Kiel, Germany
[8]Volcanic Basin Petroleum Research (VBPR), Oslo Innovation Center, Oslo, Norway

HHS, 0000-0002-4370-1179

On its way to the surface, the Siberian Traps magma created a complex sub-volcanic plumbing system. This resulted in a large-scale sill emplacement within the Tunguska Basin and subsequent release of sediment-derived volatiles during contact metamorphism. The distribution of sills and the released sediment-stored gas volume is, however, poorly constrained. In this paper, results from a study of nearly 300 deep boreholes intersecting sills are presented. The results show that sills with thicknesses above 100 m are abundant throughout the upper part of the sedimentary succession. A high proportion of the sills was emplaced within the Cambrian evaporites

with average thicknesses in the 115–130 m range and a maximum thickness of 428 m. Thermal modelling of the cooling of the sills shows that the contact metamorphic aureoles are capable of generating 52–80 tonnes of CO_2 m^{-2} with contributions from both marine and terrestrial carbon. When up-scaling these borehole results, an area of 12–19 000 km^2 is required to generate 1000 Gt CO_2. This represents only 0.7–1.2% of the total area in the Tunguska Basin affected by sills, emphasizing the importance of metamorphic gas generation in the Siberian Traps. These results strengthen the hypothesis of a sub-volcanic trigger and driver for the environmental perturbations during the End-Permian crisis.

This article is part of a discussion meeting issue 'Hyperthermals: rapid and extreme global warming in our geological past'.

1. Introduction

The emplacement of the Large Igneous Provinces (LIPs) coincides in time with several of the most severe crises and hyperthermals from the history of the Earth, such as the Paleocene Eocene thermal maximum, the Toarcian, the End-Triassic and the End-Permian (e.g. [1]). Within many of the LIPs, not only there is a large outpouring of volcanics at the surface, there is also a significant sub-volcanic component, with magma having intruded into sedimentary rocks as sills, dykes and volcanic centres (e.g. [2–4]). Gas release directly from the igneous rocks (CO_2 and SO_2), and at contact aureoles around intrusions, such as sills (CO_2, CH_4, CH_3Cl, CH_3Br and CO_2), may explain rapid global warming and other perturbations such as ozone layer destruction (e.g. [5–10]). Here, the Siberian Traps and the End-Permian crisis are used as an example of how LIPs and environmental crises may be causally linked, with specific focus on the potential for gas generation in the metamorphic contact aureoles in the sedimentary rocks around the sub-volcanic intrusions.

The Siberian Traps LIP (figure 1) is one of the world's largest LIPs, with outcrops and subcrops widespread in the Northwestern Siberian craton, including the Taimyr Peninsula to the north and below the West Siberian basin to the west. The volume of igneous rocks is estimated to be a minimum of 1.7 M km^3 [12] with the main pulse of emplacement taking place through the Tunguska Basin in East Siberia around 252 Ma (e.g. [13,14]). Sills and dykes are abundant throughout the basin and form sheets up to at least 350 m thickness, locally comprising up to 65% of the basin stratigraphy [15,16] with a maximum cumulative sill thickness of 1200 m [17]. Some examples of the thick sheet sills outcropping in coal-bearing sedimentary rocks are given in figure 2.

Degassing of sediment-stored volatiles from the Tunguska Basin following magma emplacement is thought to be of the order of 100 000 Gt CO_2 [7], coinciding in time with the End-Permian negative carbon isotope excursion [14]. There is evidence of numerous pipe and vent structures throughout the basin (e.g. [18]; see distribution in figure 1), which indicate that catastrophic gas escape occurred at a large number of sites during the emplacement of the Siberian Traps [7]. Individual sills may have reached volumes of greater than 5000 km^3, potentially resulting in decadal-scale climate change [19] following the release of the gases to the atmosphere. Moreover, evaporite and coal metamorphism around the sills likely mobilized additional C, Cl and Br (e.g. [7,8]), adding to the environmental stress. However with outcrop examples (e.g. Figure 2) being very limited over the vast size of the area, the distribution of sills in the Tunguska Basin is still poorly documented. This makes detailed and realistic assessments of the role of sills in the End-Permian event challenging. Only a handful of borehole logs are available in the international scientific literature, usually with limited lithological information (e.g. [12]). To help address this data gap, we use a large petroleum industry borehole database in combination with a thermal model to better quantify the gas generation following sill emplacement during the Siberian Traps LIP.

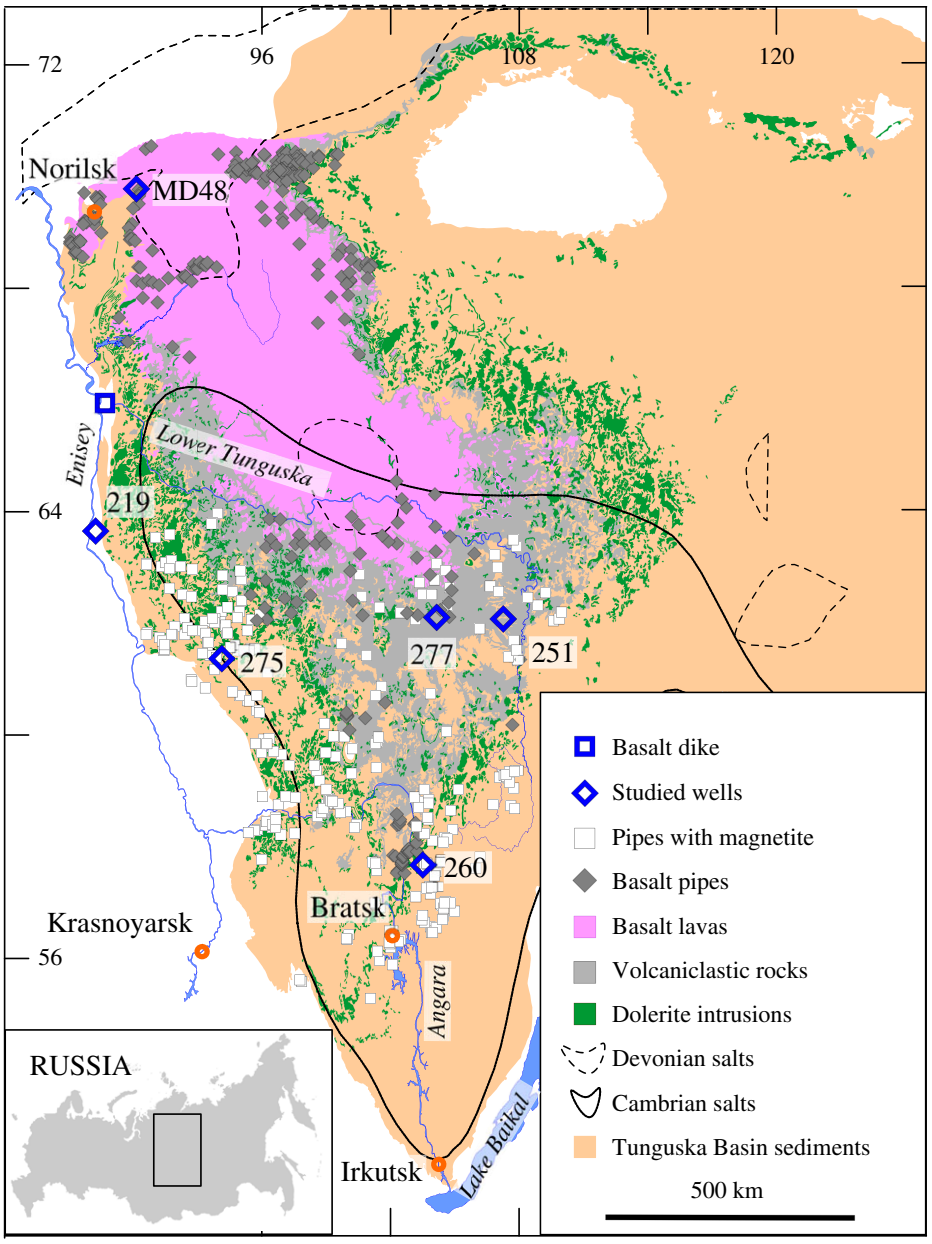

Figure 1. Simplified geological map of the Siberian Traps and the Tunguska Basin. Note that the 'Tunguska Basin' in the literature is frequently included in the terms 'Siberian Platform' and 'Siberian Craton', and that the Tunguska Basin is often considered as one of many basins situated on the platform/craton. We use the term 'Tunguska Basin' to encompass all the post Neo-Proterozoic sedimentary rocks on the platform/craton, and refer to the various provinces and structures following the nomenclature of [11]. In addition, Russian geologists often use the term 'synclise' instead of 'basin', as shown in [11]. (Online version in colour.)

2. Sedimentary and volcanic rocks in the Tunguska Basin

The vast Tunguska Basin in eastern Siberia contains the oldest petroleum system in the world formed during maturation of 1–8 km thick deposits of Neo-Proterozioc shale and carbonate (e.g. [15,20,21]). The total thickness of the basin stratigraphy commonly varies between 3 and

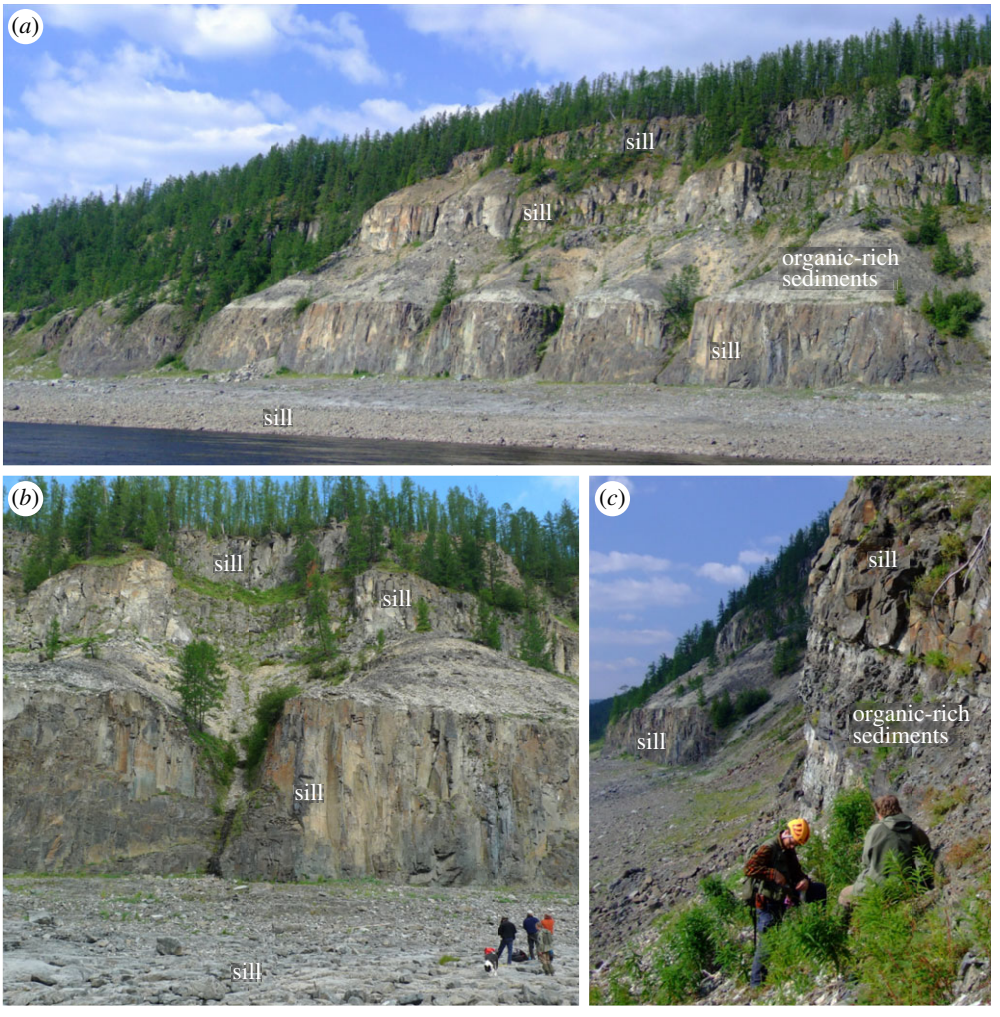

Figure 2. Outcrop examples of large sills in Siberia. (*a*) Overview of a lower Tunguska river section outcrop with sills and sediment highlighted. (*b*) At least four thick sills are clearly visible as steps in the outcrop (many smaller sills can be found on closer inspection within the sediments). (*c*) The contact of the sills with organic-rich sediments (coal) reveal metamorphic aureoles due to baking from the sill intrusions, a process which liberates gases from the host rocks. (Online version in colour.)

12.5 km depending on location [15,17] (figure 3*b*). Carbonates (with minor sandstone and shale horizons) dominate the Cryogenian and Tonian (formerly Riphean) source rock sequences which are overlain by the carbonate and evaporate facies of the Ediacaran (formerly Vendian) [11,22,23]. Furthermore, enormous volumes of Cambrian evaporites are present in the basin with up to 2.5 km thick sequences of halite-rich strata, anhydrite and dolostone (figure 3*b*) [24,25]. Five major phases of salt deposition occurred in the Cambrian, the most extensive being the 2 million km^2 Early Cambrian Usolye salt basin with an average of 200 m of nearly pure halite [24]. Most of the petroleum reservoirs are located in the Cambrian carbonates (e.g. [23]). The post-Cambrian stratigraphy contains major erosional breaks. Devonian rocks are rare in the south but abundant in the north, whereas Ordovician rocks (limestones, marls) are locally abundant in the central parts of the basin.

Sedimentation in the basin terminated in the latest Permian with the onset of the Siberian Traps extrusive volcanism. The exposed distribution of the volcanics is shown in figure 1. Lava flows do not outcrop south of approximately 60° and the absence of lava within the crater-lake deposits

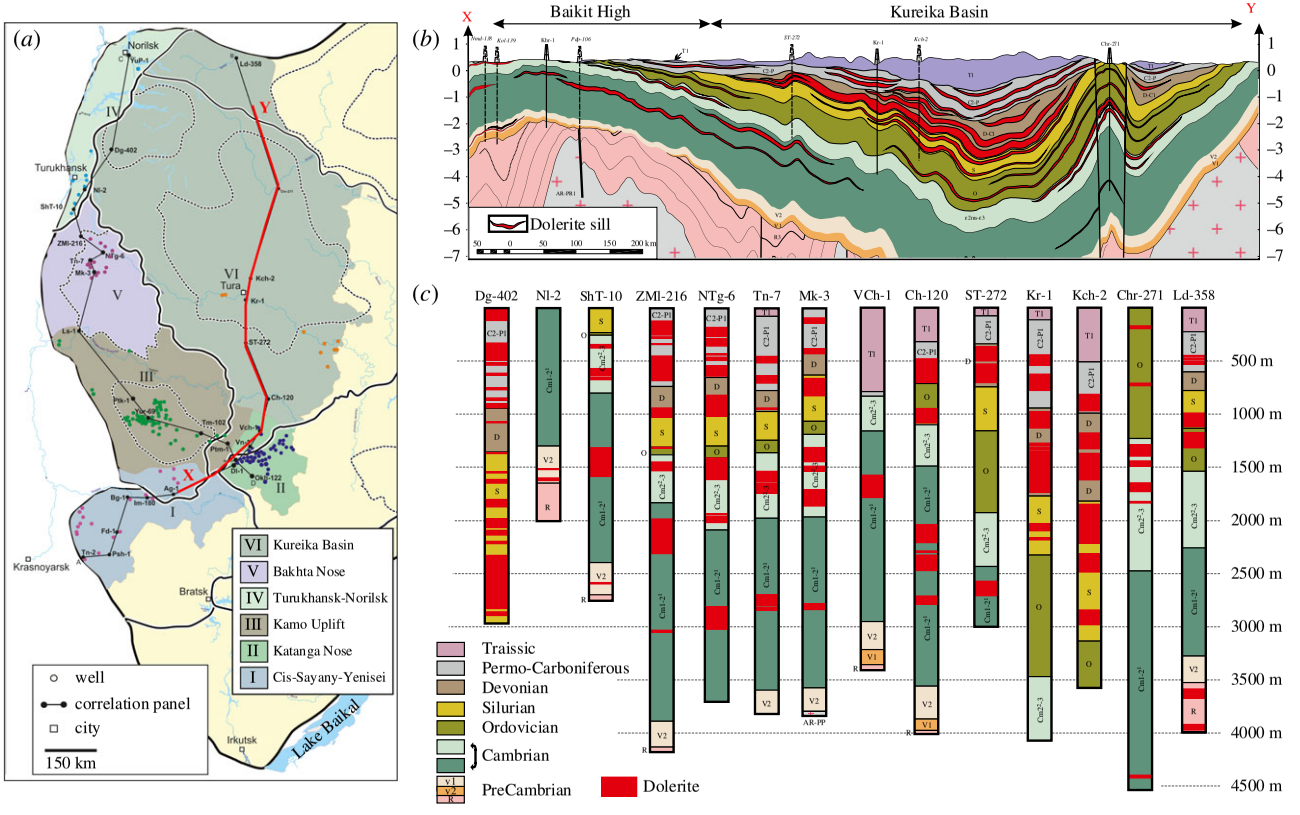

Figure 3. (*a*) Overview of the boreholes used for sill statistics and the regions I–IV. The circle fill is coloured according to the region. The red line shows the location of the composite profile in (*b*). (*c*) The logs of 15 selected boreholes along the profile (correlation panel). Note the presence of thick Devonian (evaporite-bearing) and Carboniferous-Permian (coal-bearing) strata north in the basin. (Online version in colour.)

above the explosion pipes (e.g. [26,27]) suggests that lava flows never formed an extensive cover in the southern parts of the basin. However, pyroclastic rocks are abundant in the interval of 68°–62° (figure 1; e.g. [16]), potentially linked to explosive eruptions from evaporite-rooted pipes [7,18,28].

Sills are present in most parts of the Tunguska Basin and are emplaced throughout the sedimentary succession from the basal Vendian carbonates and clastic lithologies to the uppermost Late Permian fluvial coal-bearing sandstones and siltstones (the Tunguska Series; e.g. figures 2 and 3). Knowledge about the sill distribution is based on outcrop studies and boreholes, and sill volume calculations are currently based on limited borehole assessments (e.g. [12]). This approach has resulted in virtually unexplored areas where the borehole coverage is poor or the boreholes are shallow. Seismic data could potentially have resolved the extent of deeply emplaced sills, but have proved to be of limited use due to imaging issues resulting from the similarities in physical properties and seismic responses between dolerite and dolostone.

Sill emplacement within the Siberian LIP led to contact metamorphism, widespread magma–sediment interactions, the formation of degassing pipes and precipitation of ores (e.g. [7,18,29–32]). The timing of sill emplacement overlaps the global negative carbon isotope excursion that characterizes the End-Permian event and is potentially preceded by the first extrusive phase [14]. The most profound results of the magma–sediment interaction are the spectacular magnetite-rich pipes rooted in the Cambrian evaporites or possibly deeper [7,18,32,33]. These degassing pipes are numerous in the southern parts of the basin (figure 1) where they are associated with up to 700 m deep and 1.6 km wide crater-lake deposits [18,26,27]. The pipes may have played a key role as degassing structures linking the Siberian Traps to the End-Permian event [7,8]. The distribution of these pipes and indeed the extent of dolerite outcrops (figure 1) indicates that the sub-volcanic parts of the Siberian trap LIP are extensive, but just how thick and widespread are the sediment-hosted sills?

3. Data and methods

Data and material from 284 parametric and petroleum exploration boreholes were used to investigate the sills emplaced in the Siberian Traps (figure 3*a*). The boreholes cover large parts of the basin, from Norilsk in the north (N 69°) to Bratsk in the south (N 55°), with a bias towards petroleum-bearing regions. The boreholes are mainly from the Krasnoyarsk Territory and are characteristic of the western half of the Tunguska Basin where volcanism was particularly widespread during the End-Permian. The main source of data was an industry catalogue available at the Moscow State University showing stratigraphic subdivisions and logs from deep wells, but additional sources were used to get good information from other territories (Turukhansk-Norilsk Range, Bakhta Nose and Kureika Basin). The boreholes were then grouped according to the six main oil-exploration zones of the Krasnoyarsk Territory. Overall, these zones match the large structural elements of the Siberian Platform (figure 3*a*): (I) 28 wells, all deeper than 1.5 km, from the north of Cis-Sayany-Yenisei Syneclise together with Angara Dislocations Zone (sometimes the former is included into Baikit High); (II) 85 wells, all deeper than 2 km, from the Katanga Nose of Nepa-Botuoba High (sometimes referred to as the Katanga Saddle) and the adjacent part of Vanavara embayment (i.e. the southwestern part of the Kureika Basin); (III) 114 wells from the Kamo Uplift of the Baikit High and the adjacent part of the Vanavara embayment, all deeper than 2 km; (IV) 16 wells from the Turukhansk-Norilsk Range, 60% deeper than 2.5 km; (V) 24 wells from the Bakhta Nose of Baikit High, all deeper than 2 km; and (VI) 17 wells from the Kureika Basin (excluding the Vanavara embayment) and the adjacent part of the Anabar High (Putoran Nose), 90% are deeper than 3 km. A selection of 14 of the logs from these areas are shown in figure 3*c* and additional boreholes are presented in the electronic supplementary material, figure S1.

Additional simplified logs from seven boreholes are compiled in figure 4, where one borehole log (MD-48) is from [31] and the rest are from the Siberian Scientific Research Institute of Geology, Geophysics and Mineral Resources, Novosibirsk.

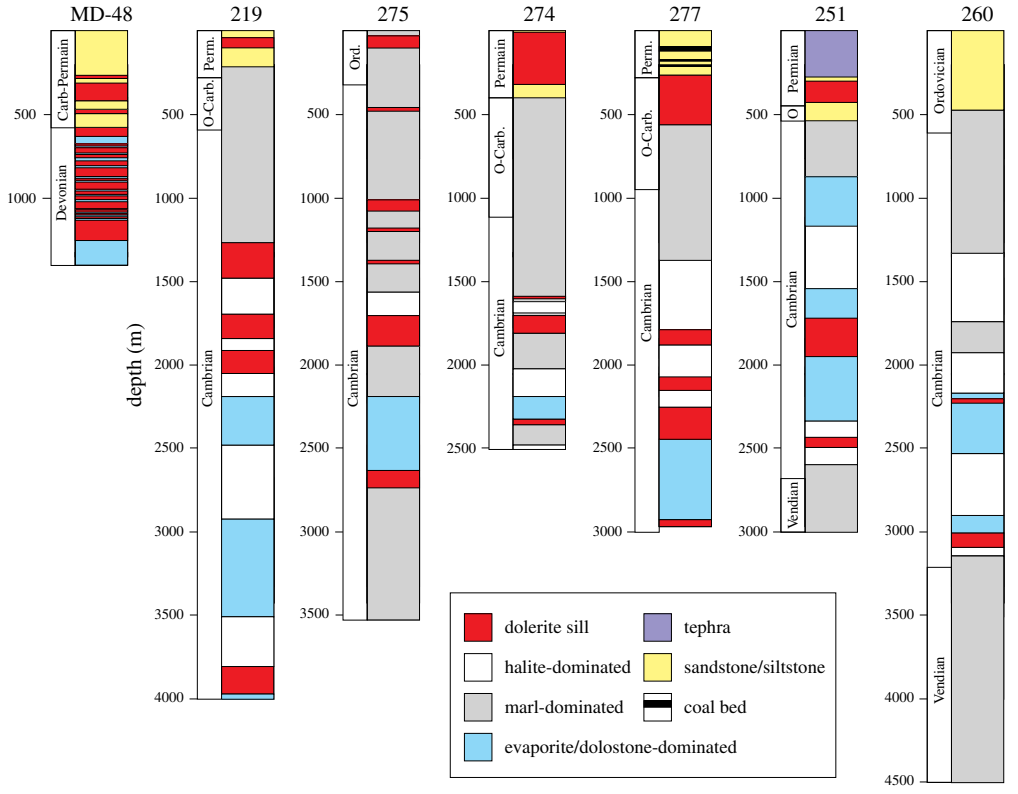

Figure 4. Logs from seven boreholes, five are from the E-W transect shown in figure 1. Three of these boreholes (219, 275, 277) are used for thermal modelling as detailed lithological logs are available. (Online version in colour.)

We have used the SILLi 1.0 1D numerical model [34] to recreate the thermal effects of sill emplacement in three selected boreholes. The general aspects of the model are described here and further details are given in [34]. First, each sedimentary layer, including eroded layers, is deposited sequentially in time based on the depositional age. The rate of sedimentation for each layer is then determined by the thickness of the layer and the difference in time between its top age and that of the layer deposited before it. A thermal solver computes the temperature within the deposited sedimentary column by applying fixed temperatures at the top and bottom at every step, calculated from the prescribed geotherm and the energy diffusion equation. In contrast to many published thermal models (e.g. [35]), this enables us to compare and separate the thermal effects of sills with the normal burial effects. Sills are emplaced instantaneously at a given time. The effective rock heat capacity accounts for the latent heat of fusion in the crystallizing parts of the sill [35–37]. Dehydration reactions in the host rocks are implemented by modifying the thermal diffusion equation when temperatures of the sediments are increasing within a certain range [36,38]. Deposition of an erosional layer occurs in the same way as the layers in the present-day sedimentary column. Erosion occurs instantly at the prescribed time and the top and bottom temperature boundary conditions are accordingly adjusted for the new sedimentary column. The EASY%Ro method [39] is used to calculate the thermal maturity of the sedimentary rocks. Organic CO_2 generated from the breakdown of organic matter is calculated from the difference in TOC content before and after sill emplacement [35], but note that the EASY%Ro method leaves 15% of the TOC behind, even close to the sill where maximum conversion occurs. The amount of inorganic carbon released during decarbonation reactions from carbonate-bearing rocks is based on interpolation on the pressure–temperature phase diagrams generated by Perple_X using pre-defined rock geochemistry for marls [40]. Note that the carbon gas speciation is calculated as CO_2-equivalents even though CH_4 is a common product of sediment metamorphism.

4. Results

The two key aspects of the sub-volcanic system that are addressed in this contribution are: (i) a better constrained account of the distribution and thickness of sill intrusions, with specific detail on the types of host sediment, and (ii) improved thermal modelling to better estimate gas outputs due to the metamorphic aureoles around the intrusions. Results from these two main aspects are described in detail below and will form the basis for the discussion sections.

(a) Sill distribution and thickness

In total, 93.5% of the 284 boreholes from the database contain sill intrusions (figure 3*c* and electronic supplementary material, figure S1), and all of the additional boreholes in figure 4. Owing to the depositional and erosional history of the Tunguska Basin, we cannot determine the potential preference for sills in specific lithologies, ages or with depth. We do not have access to the thickness variations along strike of individual sills in the database. However, as shown in the geological profile in figure 3*b*, there are abundant and thick sills in the central parts of the basin, in particular in post-Ordovician strata (cf. figure 5). The thickest average sills are emplaced in the marl-bearing Ordovician in area III (the Kamo Uplift of the Baikit High; 190 m), whereas sills are generally thick in the Cambrian evaporites across the basin as well. The thickest individual sill in the presented logs is 428 m (borehole ZMI-216), emplaced in Cambrian strata. In areas I, II and IV, the thickest sills (on average) are within the Cambrian (figure 5), even when considering that we have subdivided the Cambrian into salt- and anhydrite-dominated evaporites (Cm2–3 ev) and dolostones (Cm1–2). Note that towards the anticline along the profile in the south (the border zone between areas I, II and III; figure 3*b*), sills are less abundant, as also demonstrated by borehole 260 in figure 4 (located near Bratsk). As shown in the log overview (figures 3*c* and 4; electronic supplementary material, figure S1) the Carboniferous to Permian sedimentary rocks, dominantly sandstone and siltstone with coal beds, are heavily intruded by sills.

The boreholes in figure 4 (excluding MD-48) contain a total of 26 sills with an average sill thickness of 120 ± 81 m. Among these logs, the thickest sill is 300 m (borehole 274), emplaced within the Permian coal-bearing Tunguska Series.

Owing to the relatively few boreholes available from areas I and IV, and the range in average sill thicknesses with basin structure, it is not possible to calculate reliable sill volumes for the entire Tunguska Basin, or the exact contributions from the various lithological units (e.g. coal versus marl metamorphism). As a consequence, estimating accurate LIP-scale degassing from contact metamorphism around the sills is still challenging. Thus, instead of calculating a full basin-scale metamorphic CO_2 production value (cf. [7]), we focus on thermal modelling of specific boreholes and the equivalent areas needed to produce 1000 Gt CO_2. The reason for choosing 1000 Gt CO_2 as a benchmark value is that it can easily be scaled to the carbon mass required to cause global changes, and that a flux of 1 Gt/yr may be obtained when generated within a realistic timeframe of contact metamorphic gas production (cf. [16,19]).

(b) Thermal modelling

As an example of our approach to calculate gas generation from contact metamorphism, we use a thermal model (see table 1 for input details) calibrated to three borehole cases (boreholes 275, 277, 219; figure 4). These boreholes intersected sills emplaced in Cambrian and younger sedimentary rocks. The model calculates the aureole temperatures, vitrinite reflectance, TOC reduction from pre-intrusion values, and the generated CO_2 from TOC and marl metamorphism. Note that the marl metamorphism releases CO_2 at temperatures primarily above *ca* 400°C due to calc-silicate reactions and is, thus, restricted to the innermost parts of the contact aureoles. The calculated TOC is compared to measured TOC where data are available. Total organic carbon (TOC) data from the six boreholes in figure 4 (not including MD48) shows that the content is generally low in evaporites and dolostones (0–0.3 wt%), with occasional high-TOC

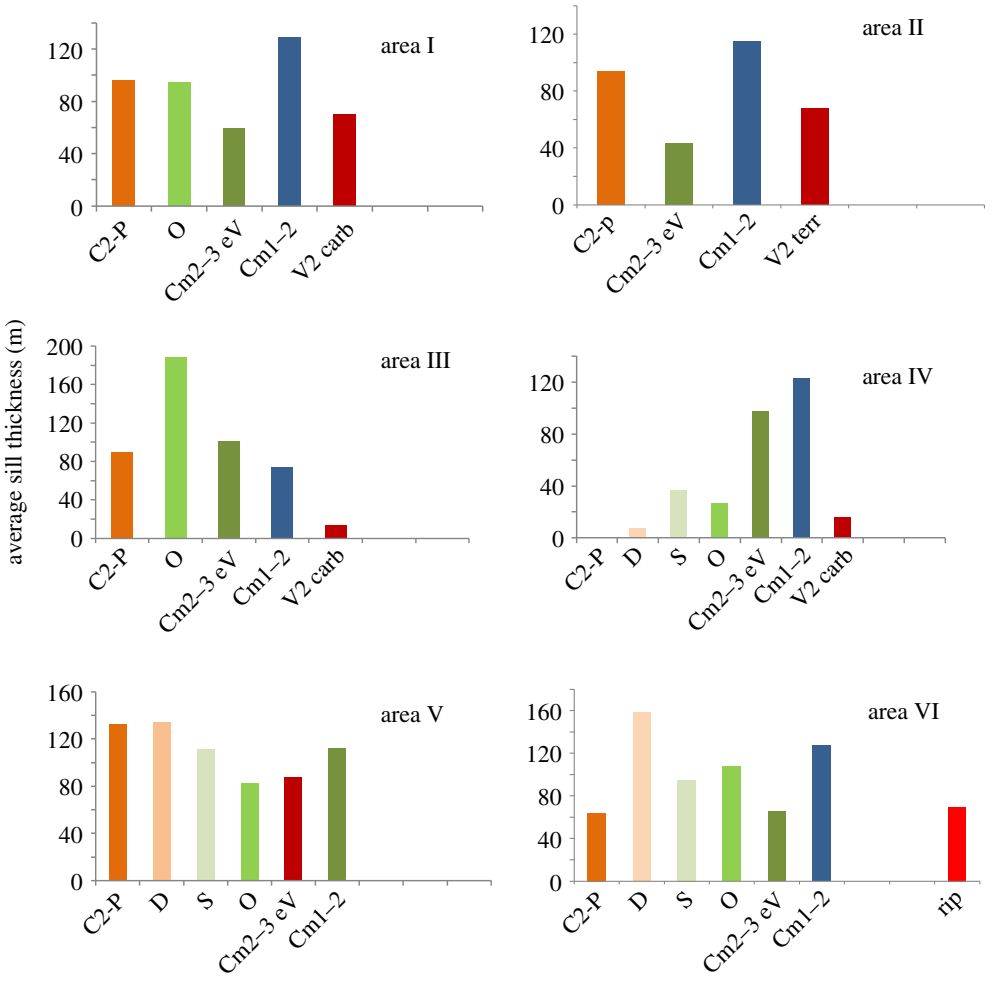

Figure 5. Average sill thicknesses in individual boreholes sorted according to the age of the enclosing sedimentary strata and the regional division from figure 2. (Online version in colour.)

shale intervals peaking at above 6 wt% (unpublished data from the Siberian Scientific Research Institute of Geology, Geophysics and Mineral Resources; electronic supplementary material, table s1). Note that the TOC values represent present-day values that were considerable higher at the time of sediment deposition and the time of sill emplacement (cf. [22]). Moreover, vitrinite reflectance measurements are not available from our boreholes. Both vitrinite and TOC borehole measurements are needed in order to more accurately calibrate the sill model, including the relative emplacement time of the sills.

The model output from borehole 219 is shown in figure 6 and demonstrates increasing vitrinite reflectance and reduced TOC near the sills. The maximum temperature obtained is about 800°C in between the closely spaced sills at 1200–2000 m. Note that if closely spaced sills are emplaced at the same time, as in the 219 case (252 Ma), the result is higher temperatures between the sills (and more CO_2 generation) compared with sills emplaced with greater than 50 000-yr spacing (cf. [41]).

The cumulative CO_2 production from the metamorphism in borehole 219 is shown in the last two panels of figure 6. In this borehole, CO_2 is only produced in the upper aureole of one sill where marl is present. The TOC-derived CO_2 is, as mentioned, generally low due to the low initial TOC content and the values are reproduced when the initial TOC in the Cambrian strata are set to 0.5 wt% TOC. The highest TOC values are within the upper 200 m of borehole 219 where the sedimentary rocks are coal-bearing. We have used 2 wt% TOC throughout the 200 m as an

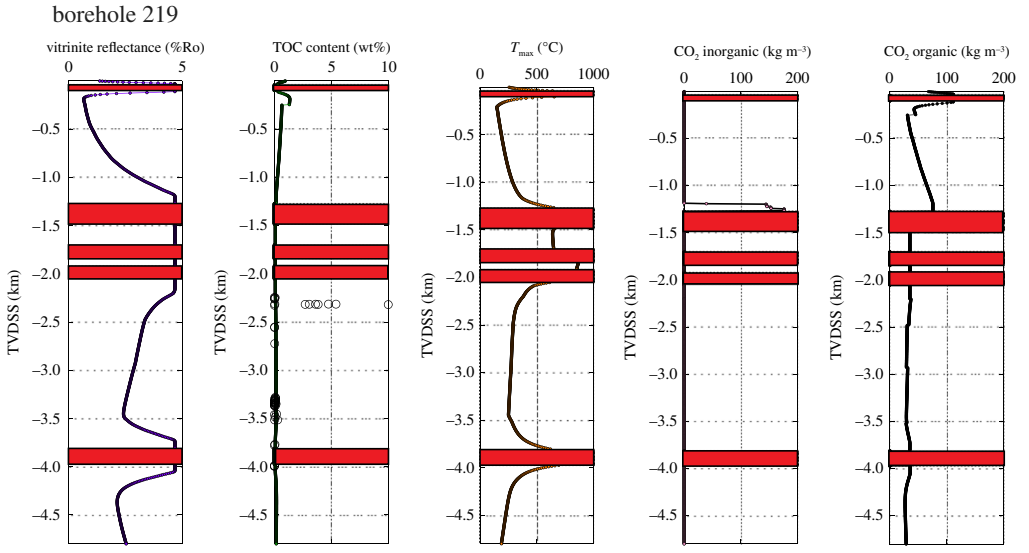

Figure 6. Thermal model results from borehole 219. Note that the high-TOC content in the 2315–2325 m interval is due to the presence of bitumen introduced during migration. (Online version in colour.)

Table 1. Rock properties.

lithology	density (kg m^{-3})	heat capacity (J kg^{-1} C^{-1})	thermal Cond. (W m^{-1} K^{-1})	latent heat Org. (kJ kg^{-1})
sandstone w/coal	2500	1000	1.8	376
shale/siltstone	2500	1000	1.8	376
dolostone	2400	1000	2.0	376
marl/limestone	2550	1000	1.8	376
halite	2650	1000	4.5	376
dolerite sill[a]	2700[b]	820/850[b]	2.1	0

[a]Includes: solidus T, 950°C; liquidus T, 1150°C; latent heat of crystallization, 375°C.
[b]Melt/solid.

approximation for a realistic bulk rock lower endmember scenario (electronic supplementary material, table s2). The results show that the cumulative CO_2 production is 40 ton m^{-2} (organic) and 12 ton m^{-2} (inorganic; table 2), with peak values reached shortly after sill emplacement (figure 7). The area needed to produce 1000 Gt CO_2 from sill metamorphism is about 19 000 km^2. The results from the two other boreholes are given in table 2 and show that 1000 Gt CO_2 is reached at 12–13 000 km^2. These areas represent 0.7–1.2% of the total area in the Tunguska Basin containing sills.

5. Discussion

(a) Sill distribution

Our data show that sills are found in all of the six regions in East Siberia and in 93.5% of the boreholes in the database. Deep boreholes without sills signify that sills may pinch out laterally. Since our database does not allow the study of individual sill thicknesses along strike, we cannot

Table 2. Inorganic- and organic-derived CO_2 generated in contact aureoles.

			sills	sills	organic	inorganic	organic	inorganic	area equals 1000 Gt CO_2	
		sills	total thickness		cumulative	production	maximum flux		aureoles	sills
borehole	name	#	m	%	ton m^{-2}	ton m^{-2}	kg m^{-2} yr^{-1}	kg m^{-2} yr^{-1}	km^2	km^2
275	Maigunnskaya	7	483	14	44	36	3265	6700	12 500	11 5022
277	Verhneilimpejskaya	5	707	24	73	4	1800	304	12 987	78 579
219	Nizhne-Imbakskaya	5	720	18	40	12	1725	720	19 231	77 160

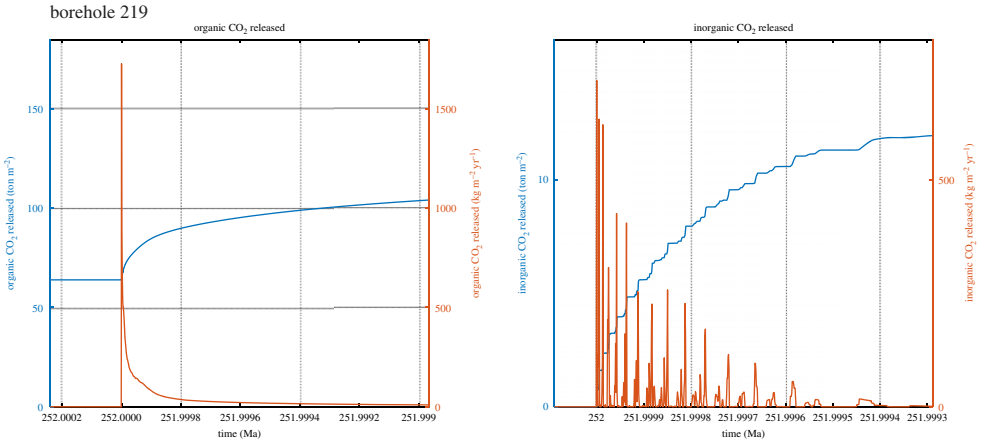

Figure 7. The thermal gas generation following metamorphism in borehole 219. The inorganic CO_2 is derived from metamorphism of impure carbonates (marl), whereas the organic CO_2 is ultimately derived from the TOC. (Online version in colour.)

determine whether very thick sills are stratigraphically associated with thin sills (offshoots) as is the case for the Karoo Basin sills in South Africa [42]. Except for the MD-48 borehole where very thin sills are repeatedly emplaced within a 1000 m thick zone, the other boreholes (figure 4) do not suggest the presence of offshoots. Very thick sills (greater than 200 m) are emplaced at all stratigraphic levels except in the Precambrian, but note the scarcity of wells penetrating such deep levels. The largest area in our study, region IV, The Kureika Basin, is also where the borehole coverage is the lowest (figure 3), showing the limits of our knowledge about the sub-volcanic domain of the Siberian Traps, in particular where the basin is deepest and the thickness of extrusives is highest.

The 27 simplified logs published by Vasiliev *et al*. [12] shows a bias towards very high sill percentages in relatively short boreholes, whereas the more representative deep boreholes have surprisingly high percentages of sills (estimated to 20–40%). Note also that the Vasiliev *et al*. (2000) logs are biased towards petroleum-producing areas and that many of the boreholes have greater than 500 m of sills in the stratigraphy, with a maximum reported individual sill thickness as high as 1180 m (emplaced within the coal-bearing Tunguska Series). Systematic studies of sill thicknesses in other sedimentary basins are few, but a recent study from the Karoo Basin shows that only four out of about 30 boreholes have greater than 500 m of sills [42]. In the Karoo case, the sills comprise less than 20–30% of the basin stratigraphy, and the borehole depth represents a major factor in the sill percentage. Short boreholes give an overestimation of the sill percentage in the basin. Biases due to short boreholes are not a problem in our East Siberia dataset, as most boreholes were drilled to 2–2.5 km depth—or deeper (including the boreholes presented in the electronic supplementary material, figure S1). The comparison between the Tunguska Basin and the Karoo Basin is interesting for several reasons and is further discussed below.

First, a significantly larger volume of melt was emplaced in the lower stratigraphic levels in the Tunguska Basin, potentially related to the type of sedimentary rocks present. The evaporites may have acted as preferred lithologies for melt accumulation and storage due to their thermal and mechanical anomalies compared with the overlying limestones and clastic sedimentary rocks. The melt accumulation in the evaporites is suggested as the main process leading to explosive pipe eruptions (e.g. [7,18,43]). In the Karoo Basin, the entire lithological column is composed of clastic sedimentary rocks. Although deep aureole degassing via breccia pipes was widespread, the pipes are much smaller than in the Tunguska Basin and are not associated with abnormal melt accumulation or unusually thick sills [44].

Second, comparisons between the Tunguska Basin and the Karoo Basin stress the role of the composition of the sedimentary rocks subjected to contact metamorphism. As pointed out a decade ago [7], the two biggest mass extinctions on record (the End-Permian and the End-Triassic) took place at the same time as sill emplacement in vast evaporite-dominated sedimentary basins. During the End-Triassic, the Central Atlantic Magmatic Province was emplaced in the onshore and evaporite-rich basins in Brazil (e.g. [10]). Moreover, sill-evaporite interactions on these scales (greater than 1 Mkm^2) are unique to the End-Permian and End-Triassic events, suggesting a causal relationship between mass extinctions and large-scale evaporite degassing [7]. The other major LIPs that are known to correlate with environmental changes, such as the Karoo LIP, the Northeast Atlantic Igneous Province and the High Arctic LIP, likely triggered rapid climatic changes and hyperthermals, but not big mass extinctions (e.g. [1]). The association between LIPs and climatic change (but not big mass extinction) is suggested to relate to CO_2 and CH_4 degassing from contact aureoles around sills emplaced in organic-rich sedimentary rocks (e.g. [6,45]). Furthermore, the emplacement of sills within predominantly sandstone-rich lithologies may even act as a sink to outgassing CO_2 from the LIP magmas, thereby reducing the possible climatic impacts [9]. This emphasizes the fundamental role of sediment composition in large-scale LIP-perturbed geochemical cycling.

(b) Sills and contact metamorphism

The emplacement of igneous sills in the Tunguska Basins led to rapid heating of the host sedimentary rocks. Dolerites have emplacement temperatures of about 1100°C and cool to background temperatures on timescales of 1000–50 000 years (figure 7), depending on a range of variables such as sill thickness, emplacement depth and thermal conductivity (e.g. [34,35,38]). During prograde heating, volatiles such as CO_2 and H_2O will be released during mineral reactions and organic matter maturation. Depending on the type of organic matter and the temperature, the heated rocks generate CO_2 and CH_4 plus higher hydrocarbon gases (e.g. [44]). In addition, depending on the temperature and initial maturity conditions, liquid hydrocarbons may have been generated further out into the thermal aureole as well, resembling natural organic maturation. Note that the innermost aureoles around thick sills are often barren of TOC (e.g. [34,41,46]), suggesting complete conversion of the TOC to gas. If the volatile production is sufficient and permeability of the system relatively low, the result may be the formation of a fracture system that expands towards the surface and eventually the formation of a pipe structure [47–50]. The pipes in the Tunguska Basin (figure 1) acted as gas transport channels connecting the deep reservoirs of volatiles with the End-Permian atmosphere [7,18].

One of the unique aspects of the geology of East Siberia is the abundance of evaporites in the contact aureoles around thick sills. Evaporites have a very high thermal conductivity (a value of 4 W/m/K is used in this study; table 1) which results in an efficient heat transport out of the sills (e.g. [10]). Heat is transferred more efficiently through salts compared to carbonates and clastic sedimentary rocks. As a result, the maximum temperatures in the contact aureoles are lower, but also the wider zones around the sills experienced elevated temperatures compared with the background geothermal gradient (figure 6). The effect of contact metamorphism of halite-rich lithologies includes grain coarsening of halite and breakdown of pyrite to iron oxides, resulting in coarse and brown evaporites close to the contacts with sills (e.g. [7,51]).

In other basins where dykes and sills have intruded into salts, sills appear to preferentially propagate laterally away from sub-vertical dykes into zones of hydrous salt such as carnalite ($KMgCl_3{\cdot}6H_2O$) (e.g. [52]). This lithological control appears primarily related to the heating and subsequent dehydration reaction of carnallite which causes the carnallite to behave as viscous fluidal horizons resulting in the non-brittle emplacement of magma and spectacular peperitic salt-magma mingling textures [52].

(c) Volatile volumes

One of the challenges in understanding the impact of sills on sedimentary basins is to estimate how many volatiles were generated during heating. The volatile budget is important for constraining fluid migration and for the fate of organic matter in sedimentary basins, but also for understanding the environmental effects in cases where gases were emitted to the atmosphere. There are several approaches to calculating gas volumes: (i) using the estimated sill volume in the entire basin and up-scaling to aureole volume (usually by using a 2 : 1 factor). If the carbon mass mobilized within the aureoles is known, the total carbon production can be calculated. This will give an estimate of the total volatile production but will not give any information about fluxes or the temporal evolution of fluid production (e.g. [6,7,46,53]); (ii) a different approach involves calculating the fluid production per individual sill and aureole [19,54]. Since the duration of sill cooling can be calculated from thermal modelling, the CO_2 fluxes can also be estimated. This approach is robust, but the total area, volume and age of individual sills are generally poorly constrained unless geophysical data and high-resolution geochronology is available; and (iii) a third approach is to calculate CO_2 production estimates from specific borehole cases following those up-scaled to relevant areas (e.g. [41]), as done in this study. Our results, as presented in figures 6 and 7 and in table 2, are the first borehole-based modelling estimates of the contact metamorphic volatile production in East Siberia during the End-Permian. The good fit between model results and borehole data (figure 6) strengthens the validity of the calculated 50–80 ton CO_2/m^2 (table 2); however, we stress that vitrinite data are not available but would have provided important additional model calibration. Vitrinite data would have given us the possibility to optimize the sill emplacement timing and to avoid too high temperatures between closely spaced sills [34,41].

The ratio of organic- to carbonate-derived CO_2 is controlled by the presence of marls in the contact aureoles and the TOC. The up-scaling from borehole to regions, where *ca.* 19 000 km^2 is needed to generate 1000 Gt CO_2 (borehole 219; table 2), is still in broad agreement with the TOC-based basin-scale estimate (i.e. approach 1 as listed above) from [7]. Since the Siberian Traps magma also contributed to the CO_2 fluxes with CO_2 degassing during ascent, we have compared our aureole estimates with the theoretical mantle-derived CO_2 degassing from the sills. When using the 18 Mt $CO_2\,km^{-3}$ value for basalt degassing from McCartney *et al*. [55], we calculate that an area of about 77 000 km^2 is needed to release 1000 Gt CO_2 using the sill volume in borehole 219 (table 2). For the three boreholes we have modelled, the aureoles may generate 4.0–9.2 more CO_2 than the sill degassing alone (table 2). We stress that our degassing estimates do not necessarily reflect the mass of gas emitted to the atmosphere. Large-scale and long-term storage of CO_2 in contact aureoles is regarded as unlikely, but the degassed versus stored mass on the timescale of the sill emplacement duration represents a poorly constrained factor.

As shown for borehole 219, 77% of the generated CO_2 is TOC-derived (table 2), the rest is sourced from limestones and marls. This implies that the exact emplacement history and timing determines the evolution of the $\delta^{13}C$ of the generated gas. Pulsed sill emplacement may thus result in pulsed degassing of TOC-derived ^{12}C-enriched CO_2 ($\delta^{13}C = -35‰$) or carbonate-derived ^{12}C-depleted CO_2 ($\delta^{13}C = 0‰$) depending on the host rock properties, as recently shown for the Central Atlantic Magmatic Province in Brazil [10].

A potentially important factor for assessing the environmental effects of the Siberian Traps not taken into account here is the involvement of gases released from pre-existing oil and gas accumulations. If sills are emplaced near petroleum reservoirs, the added heat may lead to enhanced gas production due to oil cracking and/or to reservoir leakage along fractures. As also shown by basin modelling studies [22], sill emplacement at 252 Ma resulted in a pulse of gas generation from the heating of source rocks and destruction of oil reservoirs [17]. Data from oils in East Siberia show the presence of polycyclic aromatic hydrocarbons suggesting interactions with the igneous/metamorphic system [56]. In the southern Tunguska Petroleum region, Kontorovich *et al.* [17] estimate that 30–35% of the Lower Cambrian sediments were heated to above 300°C

following sill emplacement, giving rise to high CO_2 and H_2S concentrations in gas reservoirs and mercaptan-bearing oils.

(d) Conclusion

- The Siberian Traps formed during the End-Permian extinction event. We present a new borehole compilation based on 284 boreholes from the Tunguska Basin in East Siberia, where 93.5% of the boreholes intersected Siberian Traps sills.
- The sills were emplaced predominantly in Cambrian evaporites and younger strata, with thicknesses in the 20–500 m range. Thick sills were also emplaced in Permian coal-bearing sedimentary rocks.
- Thermal one-dimensional modelling of three borehole cases shows that metamorphism of marls and rocks containing organic matter (including coal) resulted in the production of CO_2, typically in the 50–80 ton CO_2 m^{-2} range.
- When up-scaling the borehole results to a gas production of 1000 Gt CO_2, only 12–19 000 km^2 is needed, a small fraction (0.7–1.2%) of the known area with sills.
- The contact metamorphism generated 4.0–9.2 times more CO_2 compared with the sill degassing (mantle CO_2) alone.
- We conclude that the sub-volcanic domains of LIPs represent a key factor linking volcanism to global environmental changes.

6. Summary

Giant magmatic events, known as LIPs, have occurred at punctuated periods in Earth's history, causing environmental disturbances and mass extinctions. The Siberian LIP, which is implicated in the End-Permian mass extinction (approx. 252 Ma), had a vastly increased gas component generated from reactions between intrusions of magma (sills) with evaporites, carbonates and organic-rich sediments. A thermal model is used to show that an area of only 12–19 000 km^2 is needed to produce 1000 Gt CO_2, only some 0.7–1.2% of the known coverage of sill intrusions, highlighting the sub-volcanic part of the LIP as a major gas contributor.

Data accessibility. Supporting data are available as electronic supplementary material.

Authors' contributions. H.H.S. designed the study, did the thermal modelling and drafted the manuscript; K.I. contributed to the thermal modelling; S.F., G.G.A., O.V.S. and N.V.M. obtained permissions for using borehole data, extracted relevant lithologies and sill statistics and made logs and maps; D.A.J. made figures and helped draft the manuscript; A.G.P. and S.P. contributed to data management and borehole information, and study design. H.H.S., D.A.J., A.G.P. and S.P. were part of a sill outcrop study from which the Siberia Photos were collected. All authors gave final approval for publication.

Competing interests. We have no financial or non-financial competing interests.

Funding. Source of funding for each author. H.H.S., D.A.J., A.G.P. and S.P.: Centre for Earth Evolution and Dynamics (CEED), University of Oslo, Norway. S.F. and G.G.A.: Department of Geology, Lomonosov Moscow State University, Moscow, Russia. O.V.S. and N.V.M.: Siberian Scientific Research Institute of Geology, Geophysics and Mineral Resources, Novosibirsk, Russia. K.I.: GeoModelling Solutions GmbH, Zurich, Switzerland, and GEOMAR, Helmholtz Centre for Ocean Research, Kiel, Germany.

Acknowledgements. We thank the Research Council of Norway for funding through its Centres of Excellence funding scheme, project number 223272, and two referees for providing valuable comments.

References

1. Bond DPG, Wignall PB. 2014 Large igneous provinces and mass extinctions: an update. The Geological Society of America. Special Paper 505.
2. Jerram DA, Widdowson M. 2005 The anatomy of Continental Flood Basalt Provinces: geological constraints on the processes and products of flood volcanism. *Lithos* **79**, 385–405. (doi:10.1016/j.lithos.2004.09.009)
3. Jerram DA, Bryan SE. 2015 *Plumbing systems of shallow level intrusive complexes. In: advances in volcanology*. Berlin, Germany: Springer.

4. Svensen HH, Torsvik TH, Callegaro S, Augland L, Heimdal TH, Jerram DA, Planke S, Pereira E. 2017 Gondwana Large Igneous Provinces: plate reconstructions, volcanic basins and sill volumes. *Geol. Soc. Lond. Spec. Publ.* **463**, 17–40. (doi:10.1144/SP463.7).
5. Beerling DJ, Harfoot M, Lomax B, Pyle JA. 2007 The stability of the stratospheric ozone layer during the end-Permain eruption of the Siberian Traps. *Phil. Trans. R. Soc. A* **365**, 1843–1866. (doi:10.1098/rsta.2007.2046)
6. Svensen H, Planke S, Malthe-Sørenssen A, Jamtveit B, Myklebust R, Eidem T, Rey SS. 2004 Release of methane from a volcanic basin as a mechanism for initial Eocene global warming. *Nature* **429**, 542–545. (doi:10.1038/nature02566)
7. Svensen H, Planke S, Polozov A, Schmidbauer N, Corfu F, Podladchikov Y, Jamtveit B. 2009 Siberian gas venting and the end-Permian environmental crisis. *Earth Planet. Sci. Lett.* **277**, 490–500. (doi:10.1016/j.epsl.2008.11.015)
8. Black BA, Lamarque J-F, Shields CA, Elkins-Tanton LT, Kiehl JT. 2014 Acid rain and ozone depletion from pulsed Siberian Traps magmatism. *Geology* **42**, 67–70. (doi:10.1130/G34875.1)
9. Jones MT, Jerram DA, Svensen HH, Grove C. 2016 The effects of large igneous provinces on the global carbon and sulphur cycles. *Palaeogeogr. Palaeoclimatol. Palaeoecol.* **441**, 4–21. (doi:10.1016/j.palaeo.2015.06.042)
10. Heimdal TH, Svensen HH, Ramezani J, Iyer K, Pereira E, Rodrigues R, Jones MT, Callegaro S. 2018. Large-scale sill emplacement in Brazil as a trigger for the end-Triassic crisis. *Sci. Rep.* **8**, 141. (doi:10.1038/s41598-017-18629-8).
11. Frolov SV, Karnyushina EE, Korobov NI, Fadeeva NP, Akhmanov GG, Krylov OV. 2008 Neoproterozoic and lower Cambrian rock complexes in central areas of the Siberian craton: their structure and petroleum prospects. *Moscow Univ. Geol. Bull.* **63**, 386–392. (doi:10.3103/S0145875208060069)
12. Vasiliev YR, Zolotukhin VV, Feoktistov GD, Prusskaya SN. 2000 Evaluation of the volume and genesis of Permo-Triassic Trap magmatism on the Siberian Platform. *Russ. Geol. Geophys.* **41**, 1696–1705.
13. Reichow MK, Saunders AD, White RV, Pringle MS, Al'Mukhamedov AI, Medvedev AI, Kirda NP. 2002 40Ar/39Ar dates from the West Siberian Basin: Siberian flood basalt province doubled. *Science* **296**, 1846–1849. (doi:10.1126/science.1071671)
14. Burgess SD, Bowring SA. 2015 High-precision geochronology confirms voluminous magmatism before, during, and after Earth's most severe extinction. *Sci. Adv.* **1**, e1500470. (doi:10.1126/sciadv.1500470)
15. Meyerhoff, A.A. 1980. Geology and petroleum fields in Proterozoic and Lower Cambrian Strata, Lena-Tunguska Petroleum Province, Easter Siberia, USSR. In *Giant Oil and Gas fields of the decade 1968–1978* (ed. MT Halbouty). Tulsa, OK: American Association of Petroleum Geologists.
16. Fedorenko V, Czamanske GK. 1997 Results of new field and geochemical studies of the volcanic and intrusive rocks of the Maymecha-Kotuy area, Siberian Flood-Basalt Province, Russia. *Int. Geol. Rev.* **39**, 479–531. (doi:10.1080/00206819709465286)
17. Kontorovich AE, Khomenko AV, Burshtein LM, Likhanov I, Pavlov AL., Staroseltsev VS. 1997. Intense basic magmatism in the Tunguska petroleum basin, eastern Siberia, Russia. *Petrol. Geosci.* **3**, 359–369. (doi:10.1144/petgeo.3.4.359)
18. Polozov AG, Svensen HH, Planke S, Grishina SN, Fristad KE, Jerram DA. 2016 The basalt pipes of the Tunguska Basin (Siberia, Russia): High temperature processes and volatile degassing to the end-Permian atmosphere. *Palaeogeogr. Palaeoclimato. Palaeoecol.* **441**, 51–64. (doi:10.1016/j.palaeo.2015.06.035)
19. Stordal F, Svensen HH, Aarnes I, Roscher M. 2017 Global temperature response to century-scale degassing from the Siberian Traps Large Igneous Province. *Palaeogeogr. Palaeoclimato. Palaeoecol.* **471**, 96–107. (doi:10.1016/j.palaeo.2017.01.045)
20. Surkov VS, Grishin MP, Larichev AI, Lotyshev VI, Melnikov NV, Kontorovich AE. 1991 The Riphean sedimentary basins of the Eastern Siberia Province and their petroleum potential. *Precambrian Res.* **54**, 37–44. (doi:10.1016/0301-9268(91)90067-K)
21. Sokolov BA, Egorov VA, Nakaryakov VD, Bitner AK, Zkukovin YA, Kuznetzov LL, Skorobogatikh PP, Zakharyan AZ. 1992 *Geological and geophysical conditions of formation of oil and gas bearing deposits in the ancient rocks of eastern siberia*. Sydney, Australia: Petroconsultants Australasia.

22. Frolov SV, Akhmanov GG, Kozlova EV, Krylov OV, Sitar KKA, Galushkin YI. 2011 Riphean basins of the central and western Siberian Platform. *Mar. Pet. Geol.* **28**, 906–920. (doi:10.1016/j.marpetgeo.2010.01.023)
23. Frolov SV, Akhmanov GA, Bakay EA, Lubnina NV, Korobova NI, Karnyushina EE, Kozlova EV. 2015 Meso-Neoproterozoic petroleum systems of the Eastern Siberian sedimentary basins. *Precambrian Res.* **259**, 95–113. (doi:10.1016/j.precamres.2014.11.018)
24. Zharkov MA. 1984 *Paleozoic salt bearing formations of the world*. Berlin, Germany: Springer.
25. Petrychenko OY, Peryt TM, Chechel EI. 2005 Early Cambrian seawater chemistry from fluid inclusions in halite from Siberian evaporites. *Chem. Geol* **219**, 149–161. (doi:10.1016/j.chemgeo.2005.02.003)
26. Fristad KE, Pedentchouk N, Roscher M, Polozov A, Svensen H. 2015 An Integrated Carbon Isotope Record of an end-Permian Crater Lake above a Phreatomagmatic Pipe of the Siberian Traps. *Palaeogeogr. Palaeoclimato. Palaeoecol.* **428**, 39–49. (doi:10.1016/j.palaeo.2015.03.010)
27. Fristad KE, Svensen HH, Polozov A, Planke S. 2017 Formation and evolution of the end-Permian Oktyabrsk volcanic crater in the Tunguska Basin, Eastern Siberia. *Palaeogeogr. Palaeoclimato. Palaeoecol.* **468**, 76–87. (doi:10.1016/j.palaeo.2016.11.025)
28. Jerram DA, Svensen HH, Planke S, Polozov AG, Torsvik TH. 2016 The onset of flood volcanism in the north-western part of the Siberian traps: Explosive volcanism versus effusive lava flows. *Palaeogeogr. Palaeoclimato. Palaeoecol.* **441**, 38–50. (doi:10.1016/j.palaeo.2015.04.022)
29. Von Der Flaass GS, Nikulin VI. 2000 *Atlas of ore field structures of iron-ore deposits*, vol. 192. Irkutsk: Irkutsk State University Publisher. [In Russian.]
30. Turovtsev DM. 2002 *Contact metamorphism of the Noril'sk intrusions*, vol. 319. Moscow, Russia: Scientific World. [In Russian.]
31. Pang K-N, Arndt N, Svensen H, Planke S, Polozov A, Polteau S, Iizuka Y, Chung S-L. 2013 A petrologic, geochemical and Sr-Nd isotopic study on contact metamorphism and degassing of Devonian evaporites in the Norilsk aureoles, Siberia. *Contrib. Mineral. Petrol.* **165**, 683–704. (doi:10.1007/s00410-012-0830-9)
32. Neumann E-R, Svensen HH, Polozov AG, Hammer Ø. 2017 Formation of Si-Al-Mg-Ca-rich zoned magnetite in an end-Permian phreatomagmatic pipe in the Tunguska Basin, East Siberia. *Miner. Deposita* **52**, 1205–1222. (doi:10.1007/s00126-017-0717-9)
33. Von der Flaass GS. 1992 Magmatic stage in evolution of the Angara-Ilim type ore-forming system. *Russ. Geol. Geophys.* **33**, 67–72.
34. Iyer K, Svensen HH, Schmid DW. 2018 SILLi 1.0: A 1D Numerical Tool Quantifying the Thermal Effects of Sill Intrusions. *Geosci. Model Dev.* **11**, 43–60. (doi:10.5194/gmd-2017-132)
35. Aarnes I, Svensen H, Connolly JAD, Podladchikov YY. 2010 How contact metamorphism can trigger global climate changes: modeling gas generation around igneous sills in sedimentary basins. *Geochim. Cosmochim. Acta* **74**, 7179–7195. (doi:10.1016/j.gca.2010.09.011)
36. Galushkin YI. 1997 Thermal effects of igneous intrusions on maturity of organic matter: A possible mechanism of intrusion. *Org. Geochem.* **26**, 645–658. (doi:10.1016/S0146-6380(97)00030-2)
37. Iyer K, Rüpke L, Galerne CY. 2013 Modeling fluid flow in sedimentary basins with sill intrusions: Implications for hydrothermal venting and climate change. *Geochem. Geophys. Geosyst.* **14**, 5244–5262. (doi:10.1002/2013GC005012)
38. Wang DY. 2012 Comparable study on the effect of errors and uncertainties of heat transfer models on quantitative evaluation of thermal alteration in contact metamorphic aureoles: thermophysical parameters, intrusion mechanism, pore-water volatilization and mathematical equations. *Int. J. Coal Geol.* **95**, 12–19. (doi:10.1016/j.coal.2012.02.002)
39. Sweeney J, Burnham AK. 1990 Evaluation of a simple model of vitrinite reflectance based on chemical kinetics. *AAPG Bull.* **74**, 1559–1570.
40. Connolly JAD, Petrini K. 2002 An automated strategy for calculation of phase diagram sections and retrieval of rock properties as a function of physical conditions. *J. Metamorph. Geol.* **20**, 697–708. (doi:10.1046/j.1525-1314.2002.00398.x)
41. Aarnes I, Svensen H, Polteau S, Planke S. 2011 Contact metamorphic devolatilization of shales in the Karoo Basin, South Africa, and the effects of multiple sill intrusions. *Chem. Geol.* **281**, 181–194. (doi:10.1016/j.chemgeo.2010.12.007)

42. Svensen HH, Polteau S, Cawthorn G, Planke S. 2016 Sub-volcanic Intrusions in the Karoo Basin, South Africa. In *Advances in volcanology* (eds C Breitkreuz, S Rocchi). Berlin, Germany: Springer.
43. Von der Flaass GS. 1997 Structural and genetic model of an ore field of the Angaro-Ilim type (Siberian Platform). *Geol. Ore Deposits* **39**, 461–473.
44. Andresen B, Throndsen T, Råheim A, Bolstad J. 1995 A comparison of pyrolysis products with models for natural gas generation. *Chem. Geol.* **126**, 261–280. (doi:10.1016/0009-2541(95)00122-0)
45. Svensen H, Jamtveit B. 2010 Metamorphic fluids and global environmental changes. *Elements* **6**, 179–182. (doi:10.2113/gselements.6.3.179)
46. Svensen H, Planke S, Chevallier L, Malthe-Sørenssen A, Corfu B, Jamtveit B. 2007 Hydrothermal venting of greenhouse gases triggering Early Jurassic global warming. *Earth Planet. Sci. Lett.* **256**, 554–566. (doi:10.1016/j.epsl.2007.02.013)
47. Planke S, Rasmussen T, Rey SS, Myklebust R. 2005 Seismic characteristics and distribution of volcanic intrusions and hydrothermal vent complexes in the Vøring and Møre basins. In *Petroleum Geology: North-western Europe and global perspectives - Proceedings of the 6th Petroleum Geology Conference* (eds AG Doré, BA Vining). London, UK: Geological Society.
48. Aarnes I, Podladchikov Y, Svensen H. 2012 Devolatilization-induced pressure build-up: Implications for reaction front movement and breccia pipe formation. *Geofluids* **12**, 265–279. (doi:10.1111/j.1468-8123.2012.00368.x)
49. Gay A, Mourgues R, Berndt C, Bureau D, Planke S, Laurent D, Gautier S, Lauer C, Loggia D. 2012 Anatomy of a fluid pipe in the Norway Basin: Initiation, propagation and 3D shape. *Mar. Geol.* **332**, 75–88. (doi:10.1016/j.margeo.2012.08.010)
50. Iyer K, Schmid DW, Planke S, Millett J. 2017 Modelling hydrothermal venting in volcanic sedimentary basins: Impact on hydrocarbon maturation and paleoclimate. *Earth Planet. Sci. Lett.* **467**, 30–42. (doi:10.1016/j.epsl.2017.03.023)
51. Grishina S, Pironon J, Mazurov M, Goryainov S, Pustilnikov A, Von der Flaas G, Guercib A. 1998 Organic inclusions in salt. Part 3. Oil and gas inclusions in Cambrian evaporite deposit from East Siberia. A contribution to the understanding of nitrogen generation in evaporites. *Org. Geochem.* **28**, 297–310. (doi:10.1016/S0146-6380(97)00131-9)
52. Schofield N, Alsop I, Warren J, Underhill JR, Lehné R, Beer W, Lukas V. 2014 Mobilizing salt: Magma-salt interactions. *Geology* **42**, 599–602. (doi:10.1130/G35406.1)
53. Aarnes I, Planke S, Trulsvik M, Svensen HH. 2015 Contact metamorphism and thermogenic gas generation in the Vøring and Møre basins, offshore Norway, during the Paleocene-Eocene thermal maximum. *J. Geol. Soc.* **172**, 588–598. (doi:10.1144/jgs2014-098)
54. Aarnes I, Fristad K, Planke S, Svensen H. 2011 The impact of host-rock composition on devolatilization of sedimentary rocks during contact metamorphism around mafic sheet intrusions. *G-Cubed* **12**, G10019. (doi: 10.1029/2011GC003636)
55. McCartney K, Huffman AR, Tredoux M. 1990 A paradigm for endogenous causation of mass extinctions, in Special Paper of the Geological Society of America, edited, 125–138. (doi:10.1130/SPE247-p125)
56. Martikhaeva DKh, Polozov AG. 2001 Organic matter from some hydrothermal deposits of Eastern Siberia. Mineral deposits at the beginning of the 21st century. Piestrzynski *et al*. (eds). Swets and Zeitlinger Publishers Lisse.